nature genetics

Mutation of the *RAD51C* gene in a Fanconi anemia–like disorder

Fiona Vaz[1,10], Helmut Hanenberg[2,3,10], Beatrice Schuster[4], Karen Barker[5], Constanze Wiek[2], Verena Erven[2], Kornelia Neveling[4], Daniela Endt[4], Ian Kesterton[6], Flavia Autore[7], Franca Fraternali[7], Marcel Freund[2], Linda Hartmann[8], David Grimwade[1], Roland G Roberts[1], Heiner Schaal[8], Shehla Mohammed[9], Nazneen Rahman[5], Detlev Schindler[4,11] & Christopher G Mathew[1,11]

Fanconi anemia (FA) is a rare chromosomal-instability disorder associated with a variety of developmental abnormalities, bone marrow failure and predisposition to leukemia and other cancers[1]. We have identified a homozygous missense mutation in the *RAD51C* gene in a consanguineous family with multiple severe congenital abnormalities characteristic of FA. *RAD51C* is a member of the RAD51-like gene family involved in homologous recombination–mediated DNA repair. The mutation results in loss of RAD51 focus formation in response to DNA damage and in increased cellular sensitivity to the DNA interstrand cross-linking agent mitomycin C and the topoisomerase-1 inhibitor camptothecin. Thus, biallelic germline mutations in a RAD51 paralog are associated with an FA-like syndrome.

FA is a highly heterogeneous disorder, arising from biallelic mutations in one of at least 13 different genes (*FANCA*, *FANCB*, *FANCC*, *BRCA2* (*FANCD1*), *FANCD2*, *FANCE*, *FANCF*, *FANCG*, *FANCI*, *BRIP1* (*FANCJ*), *FANCL*, *FANCM* and *PALB2* (*FANCN*); ref. 1). A key step in the FA pathway is monoubiquitination of FANCD2 and FANCI, which requires the presence of a core complex of FA and FA-associated proteins. This post-translational modification is intact in FA groups D1, J and N, which therefore appear to function downstream of the core and I-D2 complexes[1]. Most individuals diagnosed with FA have germline defects in one of the known FA genes. However, identification of the causal genetic defects in the small minority of individuals with unclassified FA may offer important insights into the function of the FA pathway in inherited disorders and cancer.

The pedigree and genetic analysis of the family investigated in this study is shown in **Figure 1** and clinical and laboratory details are summarized in **Table 1**. The parents of the affected children are first cousins of Pakistani origin (**Fig. 1a**). A daughter (IV-3) died at 2 months of age with multiple congenital abnormalities, including one absent and one vestigial thumb, a congenital heart defect, imperforate anus and hydronephrosis. Her lymphocytes showed elevated chromosome breakage after treatment with the DNA interstrand cross-linking (ICL) agent mitomycin C (MMC), indicating a diagnosis of FA. A son (IV-2) died 2 d after birth with congenital abnormalities similar

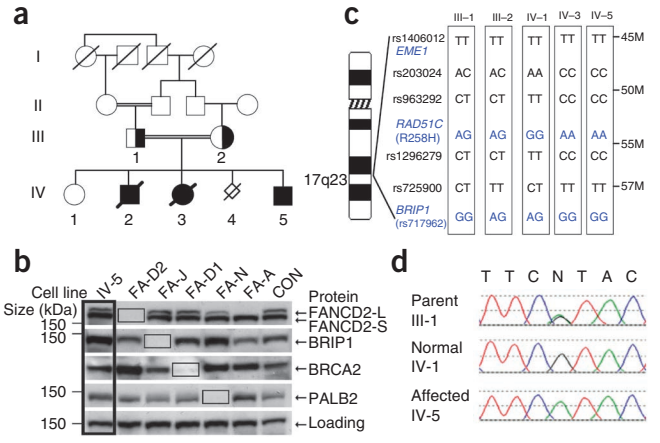

Figure 1 Genetic analysis of the family carrying an FA-like disorder. (**a**) Pedigree of the family. (**b**) Protein blot of fibroblasts from subject IV-5 and of other FA cell lines (FA-D2, FA-J, FA-D1, FA-N and FA-A denote lines with mutations in *FANCD2*, *BRIP1*, *BRCA2*, *PALB2* and *FANCA*, respectively); ubiquitinated FANCD2 (FANCD2-L) and nonubiquitinated FANCD2 (FANCD2-S) and other downstream FANC proteins are present in cells from IV-5. CON, unaffected control; loading control is RAD50. (**c**) Linkage analysis with SNPs on chromosome 17q23. M, megabases. The first fully informative SNP rs203024 is distal to *EME1*. (**d**) Sequencing of the mutation in *RAD51C* (G773A) in family members.

[1]Department of Medical and Molecular Genetics, King's College London School of Medicine, Guy's Hospital, London, UK. [2]Department of Pediatric Hematology, Oncology and Clinical Immunology, Children's Hospital, Heinrich Heine University, Düsseldorf, Germany. [3]Department of Pediatrics, Wells Center for Pediatric Research, Riley Hospital, Indiana University School of Medicine, Indianapolis, Indiana, USA. [4]Department of Human Genetics, University of Würzburg, Würzburg, Germany. [5]Section of Cancer Genetics, Institute of Cancer Research, Sutton, Surrey, UK. [6]Cytogenetics Laboratory, Genetics Centre, Guy's and St. Thomas' NHS Foundation Trust, Guy's Hospital, London, UK. [7]Randall Division of Cell and Molecular Biophysics, King's College London, New Hunt's House, Guy's Hospital, London, UK. [8]Institute of Virology, Heinrich Heine University, Düsseldorf, Germany. [9]Department of Clinical Genetics, Guy's and St. Thomas' NHS Foundation Trust, Guy's Hospital, London, UK. [10]These authors contributed equally to this work. [11]These authors contributed equally to the direction of this work. Correspondence should be addressed to C.G.M. (christopher.mathew@genetics.kcl.ac.uk), H.H. (helmut.hanenberg@uni-duesseldorf.de) or D.S. (schindler@biozentrum.uni-wuerzburg.de).

Received 9 November 2009; accepted 22 March 2010; published online 18 April 2010; doi:10.1038/ng.570

Table 1 Clinical and laboratory data for siblings family

Sibling gender	Clinical phenotype	Status	Chromosome breakage[a]
IV-1 Female	No features of FA	Well, aged 22 years	Blood lymphocytes IV-1: 0.01 (Sp); 0.03 (MMC) Control: 0.02 (Sp); 0.06 (MMC) Conclusion: normal
IV-2 Male	Intestinal, anal and respiratory abnormalities	Died age 2 d	Not done
IV-3 Female	Absent and vestigial thumb Severe congenital heart disease Hydronephrosis Imperforate anus	Died age 2 months	Blood lymphocytes IV-3: 0.07 (Sp); 0.90 (MMC); 17 multiradials in 80 metaphases Control: 0.02 (sp); 0.06 (MMC) Conclusion: elevated
IV-4	Unknown	Miscarriage at 11 weeks	Not done
IV-5 Male	Bilateral radial hypoplasia Long, slim fingers with proximally placed thumbs Hypoplastic thenar eminences Bilateral cystic kidneys Duodenal web Anal/rectal atresia Mild hypothyroidism Undescended testes Small genitalia	10 years old	Blood lymphocytes 0.12 (Sp); 0.38 (DEB); 5 multiradials in 100 metaphases Control: 0.0 (Sp), 0.04 (DEB) Fibroblasts IV-5: 0.15 (Sp); 1.24 (MMC) Control: 0.03 (Sp); 0.09 (MMC) Conclusion: elevated

[a]Mean breaks per cell occurring either spontaneously (Sp) or induced by MMC or DEB. Rates of multiradials were observed in stressed cultures.

to IV-3, and a fourth pregnancy (IV-4) miscarried at 11 weeks. The youngest child (IV-5), now aged 10 years, has extensive congenital abnormalities including short stature, bilateral radial hypoplasia, anal atresia, bilateral cryptorchidism, small genitalia, bilateral cystic dysplasia of the kidneys and chronic renal failure. Chromosome breakage testing of primary cultured fibroblasts showed clearly elevated breakage after exposure to MMC and diepoxybutane (DEB; **Fig. 2a** and **Table 1**), and cell cycle analysis of primary lymphocytes and cultured fibroblasts showed pronounced arrest in G2 after MMC treatment (**Fig. 2b**,**c**). The diagnosis of FA in this family was based on the presence of characteristic congenital abnormalities and the elevated sensitivity of cells from the siblings IV-3 and IV-5 to ICL agents. The only surviving affected child (IV-5) has not developed hematological abnormalities or cancer by age 10 years. In the absence of hematological symptoms thus far, we will refer to the clinical phenotype in this family as a Fanconi anemia–like disorder. However, the age of onset of these features in FA is variable, and cumulative incidence data from North American and German Registries indicate that by age 10 only 30–35% of individuals with FA have bone marrow failure, and less than 3% have developed leukemia or solid tumors[2].

Transduction of primary fibroblasts from IV-5 (SH2038-F) with retroviral vectors containing the *FANCA*, *FANCB*, *FANCC*, *FANCE*, *FANCF*, *FANCG* or *FANCL* complementary DNAs did not complement G2 arrest (data not shown). Protein blotting showed that FANCD2 and its monoubiquitinated form were present, suggesting a downstream defect in the FA pathway, and also confirmed the presence of the BRCA2, BRIP1 and PALB2 proteins (**Fig. 1b**). Sequencing of the exons and adjacent splice sites of the *BRIP1*, *BRCA2* and *PALB2* genes detected only known noncoding or synonymous polymorphisms. These data indicated that the family was likely to have a mutation in the FA/BRCA pathway in a previously unrecognized gene that functions downstream of the FA core and I-D2 complexes.

We genotyped DNA from the parents, the unaffected daughter (IV-1), and the two affected children (IV-3 and IV-5) on the Affymetrix 10K SNP array to search for candidate regions containing the causal gene by autozygosity mapping (Online Methods). The affected siblings showed seven substantial regions of shared homozygosity (>3 Mb) for which the unaffected sibling either was heterozygous or was homozygous for the opposite allele (**Supplementary Table 1**). The largest of these was a 14.6-Mb region on chromosome 17q21–q24 that was of particular interest (**Fig. 1c**), as it contained three genes involved in DNA repair (*EME1*, *RAD51C* (*RAD51L2*) and *BRIP1*) for which loss of function is associated with hypersensitivity to DNA interstrand cross-linking agents[3,4]. Sequencing of the coding regions of *EME1* in the index case (IV-5) revealed heterozygosity for multiple common intragenic polymorphisms, consistent with the fact that *EME1* is actually located 1.6 Mb proximal to the first fully informative SNP in this region (rs203024; see **Fig. 1c**). The region of linkage includes *BRIP1* (haplotype formed by SNPs rs725900 and rs717962), but this gene had already been excluded through protein blotting and sequencing (see above). Sequencing of the nine exons and splice sites of the *RAD51* paralog *RAD51C* in IV-5 revealed homozygosity for a mutation (G773A) in exon 5, which results in the amino acid substitution R258H (**Fig. 1d**). The other affected sibling (IV-3) was also homozygous for this mutation; the parents were heterozygous, and the child without FA-like abnormalities and with normal ICL sensitivity (IV-1) was homozygous for the wild-type sequence. The mutation was not present in 47 regionally and ethnically matched controls from the Lahore region of Pakistan. Sequencing of *RAD51C* coding regions in 21 subjects with FA excluded from the known complementation groups with intact FANCD2 monoubiquitination did not detect any additional mutations. The potential functional importance of the R258H mutation is supported by the fact that the arginine residue is conserved in RAD51C proteins from a wide range of species, including chicken, zebrafish, sea urchin and thale cress, and is also conserved in RAD51 itself and in two of the RAD51-like proteins, RAD51B (RAD51L1) and XRCC3 (**Supplementary Fig. 1**).

To determine whether R258H was the causal mutation in this family, we transduced primary fibroblasts from subject IV-5 (SH2038-F) with a retroviral vector containing wild-type *RAD51C* cDNA, the $RAD51C_{G773A}$ mutant, or a control vector transferring either the neomycin phosphotransferase II (*nptII*) or the puromycin N-acetyl-transferase (*pac*) gene, selected the cells in G418 or puromycin and analyzed cell cycle distributions after exposure of cells to 36 nM MMC for 48 h (Online Methods and **Supplementary Fig. 2**). The results showed that G2 arrest of the affected individual's fibroblasts was rescued specifically by expression of the wild-type *RAD51C* (**Fig. 2c**,**d**) but not by vector-mediated overexpression of the $RAD51C_{G773A}$ mutant cDNA (**Fig. 2e**). We also tested the effect of the mutation by expressing the wild-type or mutant RAD51C in two other eukaryotic cell lines that are deficient in the RAD51C protein. The hamster cell line irs3 has a splice-site mutation in *Rad51c* that causes skipping of exon 6 (ref. 5). We performed cell cycle analysis after MMC challenge of irs3 cells that had been transduced with retroviral vectors containing either the human wild-type or the mutant $RAD51C_{G773A}$ cDNA. The results (**Fig. 2f–h**) demonstrated that whereas the wild-type protein restored MMC resistance in irs3 cells, expression of the mutant protein resulted in only a modest degree of correction of cross-linker sensitivity when compared to transduction with the control vector. This suggests that R258H is a hypomorphic mutant, at least in the context of this cell line

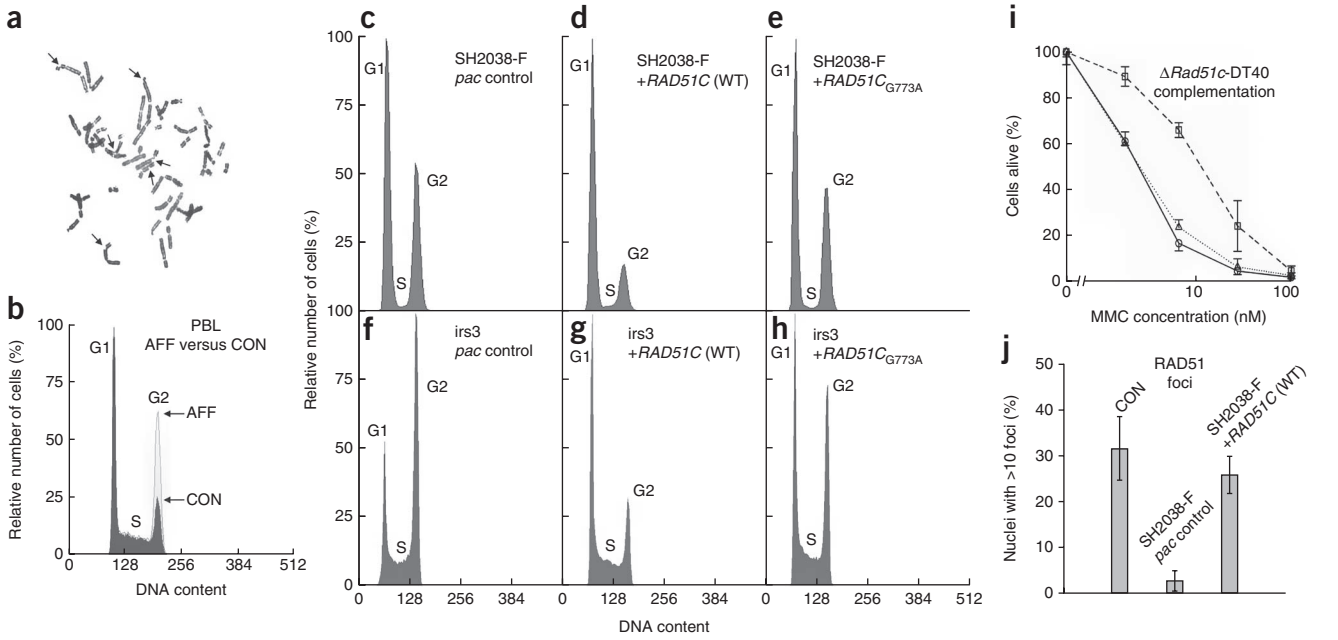

Figure 2 Functional analysis of the RAD51C alleles. (**a**) Fibroblast metaphase after exposure of the culture to 10 ng/ml MMC shows chromatid-type breakage and a radial rejoining figure (arrows). (**b**) Cell cycle distribution of peripheral blood lymphocyte culture from subject IV-5 shows increased G2 arrest (37.4% of cells in G2) in response to 45 nM MMC (AFF, light gray) compared to an unaffected control (18.4%; CON, dark gray overlay). (**c**) Untransduced (not shown) or *pac* (mock)-transduced fibroblasts from subject IV-5 (SH2038-F) show elevated G2 phase arrest (47.3 ± 8.5%, $n = 4$ experiments) after exposure to 36 nM MMC. (**d**) Transduction of SH2038-F cells with wild-type (WT) *RAD51C* rescues G2 arrest (22.6 ± 0.6%, $n = 4$, $P < 0.005$) under the same conditions as in **c**. (**e**) Transduction with mutant $RAD51C_{G773A}$ leads to a marginal decrease in G2 arrest (41.5 ± 2.3%, $n = 4$, not significant compared to mock transduction, $P = 0.24$). (**f**) Untransduced (not shown) or *pac*-transduced Rad51c-deficient hamster irs3 cells show elevated G2 phase arrest (42.5 ± 3.5%, $n = 3$) after exposure to 36 nM MMC. (**g**) Transduction of irs3 cells with human wild-type *RAD51C* rescues G2 arrest (16.4 ± 0.6%, $n = 3$, $P < 0.001$) under the same conditions as in **f**. (**h**) Transduction with mutant $RAD51C_{G773A}$ leads to a moderate decrease in G2 arrest (30.5 ± 2.7%, $n = 3$, $P < 0.005$) compared to mock transduction. (**i**) Increased survival rates indicate successful complementation of *ΔRAD51C*-DT40 chicken cells by human wild-type *RAD51C* (dashed line) but not by the mutant $RAD51C_{G773A}$ (dotted line); the solid line is from uncorrected cells transduced with control vector. Error bars are s.d. from three experiments. (**j**) SH-2038 fibroblasts from subject IV-5 are defective in the formation of RAD51 nuclear foci after exposure to MMC (2.8 ± 2.2% positive cells, $n = 4$). Transduction with wild-type *RAD51C* rescued their proficiency (25.9 ± 4.0% positive cells, $n = 4$, $P < 0.001$) to a degree that was similar to unaffected control (CON) fibroblasts (31.6 ± 6.9% positive cells). Error bars, s.d.

and the cell cycle assay. The effect of the mutation was also tested in chicken Δ*RAD51C*-DT40 cells in which the *RAD51C* ortholog is disrupted by recombination[6]. Expression of human wild-type RAD51C complemented the sensitivity of *RAD51C*-mutant cells to MMC, whereas expression from the human *RAD51C* cDNA with the G773A mutation did not (**Fig. 2i**). The specificity of correction of the MMC-sensitive phenotype was confirmed further by the finding that expression of wild-type *RAD51C* cDNA in 18 FA cell lines from different upstream and downstream complementation groups did not rescue the characteristic G2 arrest in any of these cell lines (data not shown). These data verify that *RAD51C* is the gene responsible for the cellular phenotype in this family and that R258H is the causal mutation. We suggest a provisional assignment for the FA in this family as FA-O.

We investigated the possible structural effect of the R258H mutation by homology-modeling the structure of RAD51C from the crystal structure of the archaeal rad51 protein of *Pyrococcus furiosus*[7] (PDB 1PZN; Online Methods). The arginine residue 258 is located on helix α13 in close proximity to helix α12 and faces residues Ser304 and Glu303 of the loop-connecting strands β5 and β6 (ref. 7). In the wild-type protein, Arg258 is in close contact (hydrogen-bond distance) with the carbonyl backbone of Glu303. Substitution of arginine with histidine in the model disrupts this interaction (**Supplementary Fig. 3**) and changes the electrostatic surface of this region from slightly positive to slightly negative. Together, these structural perturbations could result in rearrangement of the neighboring secondary structure elements, with relative displacement of the N-terminal and ATPase domains, and thus may affect higher-order structures such as the heptameric ring described for archaeal rad51 (ref. 7). The mutation does not appear to have a major effect on the stability of the protein, as the protein was readily detectable in the affected individual's fibroblasts on protein blots (data not shown).

As the loss of functional RAD51C protein in eukaryotic cells is associated with impaired formation of RAD51 foci in response to DNA damage[4–6], we looked for this phenotype in cells from subject IV-5. We found that RAD51 focus formation in response to MMC treatment was greatly reduced in the affected individual's fibroblasts and that this defect was corrected by transduction with wild-type *RAD51C* (**Fig. 2j**). This result strongly supports the genetic and functional complementation data that identified loss of RAD51C function as the primary defect in this family. The effect of the *RAD51C* mutation on RAD51 focus formation is shared with two of the downstream FA complementation groups, FA-D1 and FA-N, caused by mutations in *BRCA2* and *PALB2*, respectively, which encode two proteins that themselves have important roles in homologous recombination–based DNA repair[8]. The loss of RAD51 focus formation in response to interstrand cross-link–induced DNA damage prompted us to test fibroblasts from subject IV-5 for sensitivity to irradiation. As found in other FA complementation groups, the cells showed only modest radiosensitivity, which was, however, complemented by transduction with wild-type *RAD51C* (**Supplementary Table 2**). We also tested lymphoblastoid cells

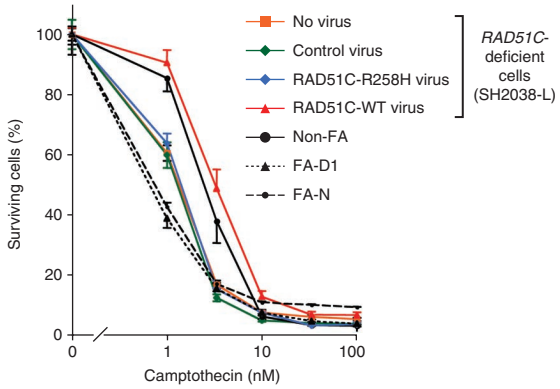

Figure 3 Camptothecin (CPT) sensitivity of lymphoblasts from subject IV-5. SH2038-L cells were tested for CPT sensitivity before transduction (no virus) or after transduction with control virus (no *RAD51C* insert), *RAD51C* with the R258H mutation, or wild-type *RAD51C*. Results for CPT-sensitive FA lymphoblastoid cell lines from FA groups FA-D1 and FA-N, and from a normal control line, are shown for comparison. The CPT sensitivity of SH2038-L is complemented by wild-type but not by mutant *RAD51C* (data shown is the mean plus or minus the one-sided s.d. from four experiments).

(SH2038-L) from the affected individual for sensitivity to the topoisomerase inhibitor camptothecin, as cells from other downstream FA groups, FA-D1 and FA-N (and FANCM-deficient cells), have recently been shown to be sensitive to this agent[9]. The *RAD51C*-deficient cells did show increased camptothecin sensitivity, which was corrected by wild-type *RAD51C* but not by cDNAs encoding the R258H mutant (**Fig. 3**). Although the camptothecin sensitivity was less marked in the affected individual's cells than in the FA-D1 and FA-N lines, these data are consistent with an FA core complex–independent role for RAD51C in addition to BRCA2, PALB2 and FANCM (ref. 9).

This study is, to our knowledge, the first report of the association of a mutation in *RAD51C* with a human disorder. The rarity of *RAD51C* mutations in humans is consistent with the fact that absence of *Rad51c* in mice causes early embryonic lethality, and there is partial embryonic lethality in *Rad51c*$^{ko/+}$ mice[10], whereas a hypomorphic *Rad51c* mouse model that expressed 5–30% of normal levels of the protein had normal growth and development but reduced fertility[11]. Thus the R258H mutation in this family may be associated with some residual function of RAD51C, as suggested by partial correction of cell cycle arrest in the hamster cell line irs3. Nonetheless, affected family members have experienced severe congenital abnormalities, some of which, such as imperforate anus and cystic kidneys with renal failure, have also been described in individuals with FA having bilateral mutations in *BRCA2* and *PALB2* (ref. 1). However, the absence of malignancies in subject IV-5 at the age of 10 years suggests that RAD51C deficiency may be associated with a less cancer-susceptible phenotype than that in the FA groups FA-D1 and FA-N.

RAD51C is known to have an important role in RAD51-mediated recombination[12,13] and recently has been shown to persist at sites of DNA damage after disassembly of RAD51 nucleoprotein filaments[14]. However, it also appears to be required for activation of the checkpoint kinase CHK2 and cell cycle arrest in response to DNA damage[14]. These characteristics suggest that *RAD51C* and the other *RAD51* paralogs may merit screening as candidate genes in families with FA-like disease and in familial cancers with undefined mutations. Indeed, in a companion paper in this issue, we demonstrate the presence of truncating and missense mutations in *RAD51C* in familial breast and ovarian cancer[15].

METHODS

Methods and any associated references are available in the online version of the paper at http://www.nature.com/naturegenetics/.

Note: Supplementary information is available on the Nature Genetics website.

ACKNOWLEDGMENTS

We thank affected individuals and their families for providing samples for this study and for donations to FA research. DNA from matched Pakistani controls was kindly provided by D.A. Khan (Department of Pathology, Army Medical College, Rawalpindi, Pakistan). We thank B. Xia (Department of Radiation Oncology, The Cancer Institute of New Jersey) for providing the PALB2 antibody, A. Sobeck for initial cloning of *RAD51C* cDNA and R. Kalb and E. Velleuer for constructing an early version of the *RAD51C* vector and for preliminary analysis. The Rad51c-deficient hamster irs3 cells were a kind gift from J. Thacker (Medical Research Council UK Radiation and Genome Stability Unit), provided by G. Illiakis (Institute of Medical Radiation Biology, University of Duisburg-Essen Medical School). We thank E. Manners for editorial assistance. We are indebted to R. Friedl for flow cytometry and to B. Gottwald and W. Kuss for expert technical assistance. Research in our laboratories was supported by the Medical Research Council UK and the Daniel Ayling Trust (F.V.), the Forschungskommission of the Heinrich Heine University, Düsseldorf (M.F., H.H.), the Deutsche Forschungsgemeinschaft SPP1230 (H.H.), the Bundesministerium für Bildung und Forschung network for congenital bone marrow failure syndromes (H.H., H.S., D.S.), the Deutsche Fanconi Anaemie Hilfe, the Aktionskreis Fanconi Anaemie and the Schroeder Kurth Fund (D.S., H.H.), the Jürgen-Manchot-Stiftung (L.H., H.S.), Cancer Research UK (K.B., N.R.) and European Molecular Biology Organization fellowship ASTF 177-2008 (F.A.).

AUTHOR CONTRIBUTIONS

The study was designed by C.G.M., D.S. and H.H. Phenotypic assessment, sample collection and characterization of FA subgroups were performed by S.M., H.H., D.S., F.V., C.G.M., I.K., C.W., B.S., V.E., K.N. and D.E. Genetic mapping, mutation analysis and functional studies were carried out by F.V., K.B., C.W., B.S., V.E., K.N., D.E., M.F. and L.H. under the supervision of H.H., H.S., D.G., D.S., N.R. and C.G.M. Bioinformatic and structural studies were done by R.G.R., F.A. and F.F. The manuscript was written by C.G.M., D.S. and H.H., with help from the other authors.

COMPETING FINANCIAL INTERESTS

The authors declare no competing financial interests.

Published online at http://www.nature.com/naturegenetics/.
Reprints and permissions information is available online at http://npg.nature.com/reprintsandpermissions/.

1. Moldovan, G.-L. & D'Andrea, A.D. How the Fanconi anemia pathway guards the genome. *Annu. Rev. Genet.* **43**, 223–249 (2009).
2. Rosenberg, P.S. *et al.* Cancer risks in Fanconi anemia: findings from the German Fanconi Anemia Registry. *Haematologica* **93**, 511–517 (2008).
3. Abraham, J. *et al.* Eme1 is involved in DNA damage processing and maintenance of genomic stability in mammalian cells. *EMBO J.* **22**, 6137–6147 (2003).
4. Godthelp, B.C. *et al.* Mammalian Rad51C contributes to DNA cross-link resistance, sister chromatid cohesion and genomic stability. *Nucleic Acids Res.* **30**, 2172–2182 (2002).
5. French, C.A. *et al.* Role of mammalian RAD51L2 (RAD51C) in recombination and genetic stability. *J. Biol. Chem.* **277**, 19322–19330 (2002).
6. Takata, M. *et al.* Chromosome instability and defective recombinational repair in knockout mutants of the five Rad51 paralogs. *Mol. Cell. Biol.* **21**, 2858–2866 (2001).
7. Shin, D.S. *et al.* Full length archaeal Rad51 structure and mutants: mechanisms for RAD51 assembly and control by BRCA2. *EMBO J.* **22**, 4566–4576 (2003).
8. Livingston, D.M. Cancer. Complicated supercomplexes. *Science* **324**, 602–603 (2009).
9. Singh, T.R. *et al.* Impaired FANCD2 monoubiquitination and hypersensitivity to camptothecin uniquely characterize Fanconi anemia complementation group M. *Blood* **114**, 174–180 (2009).
10. Kuznetsov, S.G. *et al.* Loss of Rad51c leads to embryonic lethality and modulation of Trp53-dependent tumorigenesis in mice. *Cancer Res.* **69**, 863–872 (2009).
11. Kuznetsov, S. *et al.* RAD51C deficiency in mice results in early prophase I arrest in males and sister chromatid separation at metaphase II in females. *J. Cell Biol.* **176**, 581–592 (2007).
12. Liu, Y. *et al.* RAD51C is required for Holliday junction processing in mammalian cells. *Science* **303**, 243–246 (2004).
13. Liu, Y. *et al.* Role of RAD51C and XRCC3 in genetic recombination and DNA repair. *J. Biol. Chem.* **282**, 1973–1979 (2007).
14. Badie, S. *et al.* RAD51C facilitates checkpoint signaling by promoting CHK2 phosphorylation. *J. Cell Biol.* **185**, 587–600 (2009).
15. Meindl, A. *et al.* Germline mutations in breast and ovarian cancer pedigrees establish RAD51C as a human cancer susceptibility gene. *Nat. Genet.* advance online publication, doi:10.1038/ng.569 (18 April 2010).

ONLINE METHODS

Samples and cell lines. The family in question was referred to the Department of Clinical Genetics at Guy's Hospital. We took blood samples and skin biopsy specimens, after obtaining informed consent for all participants and ethical board approval (07/Q0702/69), to test for chromosome breakage, to obtain genomic DNA and to generate cell lines. Fibroblasts (SH2038-F) were grown from pieces of the skin explant, and a lymphoblast cell line (SH2038-L) was established by *ex vivo* EBV transformation of B lymphocytes. Since the family originated from the Lahore region of Pakistan, we obtained a panel of 47 control DNAs established by the Department of Pathology at the Army Medical College (Rawalpindi, Pakistan) to test for the presence of the *RAD51C* R258H mutation. ΔRad51c-DT40 cells were purchased from the Riken BRC Cell Bank. Rad51c-deficient irs3 cells were kindly provided from J. Thacker[5] by G. Illiakis.

Chromosome breakage test. Chromosome breakage analysis was performed according to established protocols[16]. Phytohemagglutinin-stimulated peripheral blood was cultured either with or without MMC at a final concentration of 30 ng/ml, or with or without DEB at a final concentration of 100 ng/ml, for 48–72 h in parallel with an identically treated healthy control sample. We analyzed the resulting metaphase spreads by light microscopy and scored them for chromosomal instability. We compared the affected individual's results with those of the control and established laboratory ranges. Cultured fibroblasts (SH2038-F) were tested similarly but using a 36-h exposure to MMC at a final concentration of 10 ng/ml.

Radiosensitivity assay. Confluent primary fibroblasts were trypsinized, centrifuged and resuspended at 2×10^5 per milliliter in MEM media. Aliquots were transferred into CryoTube vials and irradiated with 1, 1.5, 2, 3, 4 or 5 Gy using a 6-MV linear accelerator (Siemens) as photon source. We plated cells in triplicate into 60-mm Petri dishes at 500–6,000 cells per dish, depending on the irradiation dose applied. Earle's MEM with 15% (vol/vol) fetal bovine serum was replaced every 3–4 d. After a growth period of 2 weeks, colonies (>20 cells) were stained with 1% (wt/vol) crystal violet in 20% (vol/vol) ethanol. Clones were counted on a projection screen. Means and standard errors of the ratio of colony number relative to the number of seeded cells were calculated individually and plotted as colony survival fraction versus radiation dosage. We derived survival data from three separate experiments. Cell lines studied were RAD51C-deficient SH2038-F cells and their RAD51C-complemented isogenic counterparts; ataxia telangiectasia Aa026 (ref. 17), DNA-ligase IV-deficient GYMN (ref. 18) and RAD50-deficient F239 (ref. 19) cell lines were included as radiosensitive controls. We fitted dose-response curves to the linear quadratic model $SF = \exp(-aX - bX^2)$, where SF is the survival fraction, X the radiation dose, and a and b are fitted parameters. We did calculations using Origin 5.0 (MicroCal Software) and generated graphs using SigmaPlot 10 (Systat Software).

Camptothecin sensitivity of RAD51C-deficient cells. The lymphoblast cell line from the index individual (SH2038-L) was transduced with control virus or vectors expressing either the wild-type *RAD51C* or the mutant *RAD51C* R258H cDNAs. G418 resistant cells (3×10^5) were exposed to increasing doses (0, 1, 3.3, 10, 33.3 and 100 nM) of camptothecin (Sigma). After 5 d the cultures were harvested, stained with propidium iodide and analyzed on a FACSCalibur flow cytometer (BD Bioscience). For each data point, we collected 10^4 events using the CellQuest software. Results are shown for three or four different experiments as mean ± s.d. Survival of SH2038-L cells was compared with that of the PALB2-deficient (FA-N) LNEY cell line[20], the BRCA2-deficient (FA-D1) FA62 cell line[21] and a normal control, LCL (ref. 22).

Cell cycle analysis. We exposed native or transduced cells to 36 nM (12 ng/ml; fibroblasts, irs3 cells) or 45 nM (15 ng/ml; blood lymphocytes, lymphoblastoid cells) MMC for 48 h, harvested them and stained them with 4′-6-diamidino-2-phenylindole (DAPI) at a final concentration of 1 μg/ml in a buffer containing 154 mM NaCl, 1 mM $CaCl_2$, 0.5 mM $MgCl_2$, 0.1 M Tris, 0.2% (wt/vol) BSA and 0.1% (vol/vol) NP40 for 30 min in the dark. Alternatively, we fixed cells with 70% (vol/vol) methanol for at least 1 h at −20 °C, resuspended them in PBS and stained them with propidium iodide at a final concentration of 50 μg/ml while treating them with 25 U/ml RNase A for 30 min at 37 °C in the dark. We recorded univariate flow histograms on an analytical, triple-laser-equipped flow cytometer (LSRII, Becton Dickinson) using 355-nm Lightwave solid-state modelock laser excitation of the DAPI dye or sapphire 488-nm solid-state laser excitation of propidium iodide. We quantified the resulting cell cycle distributions, reflecting cellular DNA content, using the MPLUS AV software package (Phoenix Flow Systems).

Phenotypic correction of FA cells by retroviral transduction. The control vector S11IN, expressing an IRES-*nptII* cassette, and the vector S11RCIN, expressing additionally wild-type *RAD51C* cDNA, were constructed using methods previously described (ref. 23 and **Supplementary Fig. 2**). We generated the S11IP and the S11RCIP vectors by replacing neomycin phosphotransferase II (*nptII*) with puromycin N-acetyl-transferase (*pac*) cDNA using standard procedures. The missense mutation encoding the G773A substitution was introduced using the QuikChange Site-Directed Mutagenesis kit (Stratagene) according to the manufacturer's instructions. Generation of stable oncoretroviral cell lines and transduction of adherent and nonadherent cells were performed as described[22,24,25]. Transduced cells were selected in G418 or puromycin for 7–14 d, challenged with MMC and then assayed by flow cytometry. We analyzed transduced human fibroblasts and irs3 cells by cell cycle analysis for rescue of G2-phase arrest as described above. We analyzed ΔRad51c-DT40 cells for survival rates after 3 d, in increasing concentrations of MMC, using propidium iodide to discriminate live cells from dead cells as described[22].

Immunoblotting. We performed immunoblots with samples containing 50 μg of total protein on 7% or 3–8% (for BRCA2) NuPage Tris-acetate polyacrylamide gels (Invitrogen). Membranes were probed with mouse monoclonal anti-FANCD2 (1:800; Santa Cruz sc-20022), rabbit polyclonal anti-BRIP1 (1:1,000; Novus NB100-416) or rabbit polyclonal anti-BRCA2 (1:500; Calbiochem PC146). Rabbit polyclonal anti-PALB2 (1:1,000) was a kind gift of B. Xia. Secondary antibodies included sheep anti-mouse IgG (GE Healthcare RPN4201) or donkey anti-rabbit IgG (GE Healthcare NA934V). We used these horseradish peroxidase–linked whole antibodies at dilutions of 1:2,000 to 1:5,000 and detected them by the chemiluminescence technique using the ECL system (Amersham).

Immunofluorescence. We analyzed the capability of SH2038-F primary fibroblasts to form nuclear RAD51 foci as follows. Cells were grown on glass slides, and subconfluent cultures were exposed to 50 ng/ml of MMC for 15 h for foci induction. The cells were fixed in 4% (vol/vol) paraformaldehyde in PBS (pH 6.8) for 15 min on ice and permeabilized with 0.5% (vol/vol) Triton X-100 in PBS for 10 min on ice. After blocking with 0.5% (vol/vol) fetal bovine serum and washing in PBS, we incubated the slides with monospecific rabbit polyclonal anti-RAD51 as the primary antibody (1:800; Abcam, ab 63801). Secondary antibody was Alexa594-conjugated goat anti-rabbit IgG (1:2,000; Invitrogen/Molecular Probes, A-11037). The cells were counterstained with DAPI in Vectorshield mounting medium (Vector Laboratories). We determined the percentage of foci-positive cells (more than ten foci per nucleus) visually on a Zeiss Axio Imager.A1 fluorescence microscope. For each experiment, 200–400 nuclei were analyzed.

SNP genotyping. We undertook genome-wide linkage analysis using the GeneChip Human Mapping 10K Array Xba 142 2.0, containing 10,204 SNP markers. The median intermarker distance was 113 kb, and the mean heterozygosity of markers was 0.38. We obtained genotypes using the Affymetrix protocol for the GeneChip Mapping 10K Xba array and images using an Affymetrix Gene Chip Scanner 3000. Affymetrix GeneChip Operating Software 1.4 software was used to obtain raw allele scores. We processed scores using Affymetrix GeneChip Genotyping Analysis Software (GTYPE) to derive SNP genotypes. Genotype calls were analyzed with AutoSNPa[26], which allows visualization of genotype data across each chromosome for rapid autozygosity mapping.

DNA sequencing. We designed primers to amplify the nine exons and intron-exon boundaries of *RAD51C*. Primers and PCR conditions are shown in **Supplementary Table 3**. For DNA sequencing of PCR products, we used the BigDye v3.1 cycle sequencing kit and a 3730XL DNA sequencer (Applied Biosystems).

doi:10.1038/ng.570

Modeling RAD51C structure. We modeled RAD51C structure by homology from the crystal structure of the archaeal Rad51 protein from *P. furiosus* (PDB 1PZN)[7]. We produced the sequence alignment used to build the model using PRALINE with the homology-extended alignment strategy[27]. We generated three-dimensional models using the MODELLER package[28]. The selected model was chosen on the basis of the MODELLER objective function's score. We obtained the *in silico* mutant R258H using the PyMOL mutagenesis tool (DeLano Scientific). To refine both the model and the *in silico* mutant, we performed energy minimizations with the GROMACS package[29] using the GROMOS96 force field[30].

URLs. PyMOL, http://www.pymol.org/.

16. Auerbach, A.D. *et al.* International Fanconi Anemia Registry: relation of clinical symptoms to diepoxybutane sensitivity. *Blood* **73**, 391–396 (1989).
17. Sandoval, N. *et al.* Characterization of ATM gene mutations in 66 ataxia telangiectasia families. *Hum. Mol. Genet.* **8**, 69–79 (1999).
18. Enders, A. *et al.* A severe form of human combined immunodeficiency due to mutations in DNA ligase IV. *J. Immunol.* **176**, 5060–5068 (2006).
19. Waltes, R. *et al.* Human RAD50 deficiency in a Nijmegen breakage syndrome-like disorder. *Am. J. Hum. Genet.* **84**, 605–616 (2009).
20. Reid, S. *et al.* Biallelic mutations in PALB2 cause Fanconi anemia subtype FA-N and predispose to childhood cancer. *Nat. Genet.* **39**, 162–164 (2007).
21. Antonio Casado, J. *et al.* A comprehensive strategy for the subtyping of patients with Fanconi anaemia: conclusions from the Spanish Fanconi Anemia Research Network. *J. Med. Genet.* **44**, 241–249 (2007).
22. Hanenberg, H. *et al.* Phenotypic correction of primary Fanconi anemia T cells with retroviral vectors as a diagnostic tool. *Exp. Hematol.* **30**, 410–420 (2002).
23. Kalb, R. *et al.* Hypomorphic mutations in the gene encoding a key Fanconi anemia protein, FANCD2, sustain a significant group of FA-D2 patients with severe phenotype. *Am. J. Hum. Genet.* **80**, 895–910 (2007).
24. Hanenberg, H. *et al.* Colocalization of retrovirus and target cells on specific fibronectin fragments increases genetic transduction of mammalian cells. *Nat. Med.* **2**, 876–882 (1996).
25. Hanenberg, H. *et al.* Optimization of fibronectin-assisted retroviral gene transfer into human CD34+ hematopoietic cells. *Hum. Gene Ther.* **8**, 2193–2206 (1997).
26. Carr, I.M. *et al.* Interactive visual analysis of SNP data for rapid autozygosity mapping in consanguineous families. *Hum. Mutat.* **27**, 1041–1046 (2006).
27. Simossis, V.A. *et al.* Homology-extended sequence alignment. *Nucleic Acids Res.* **33**, 816–824 (2005).
28. Martí-Renom, M.A. *et al.* Comparative protein structure modeling of genes and genomes. *Annu. Rev. Biophys. Biomol. Struct.* **29**, 291–325 (2000).
29. Berendsen, H.J.C. *et al.* GROMACS: a message-passing parallel molecular dynamics implementation. *Comput. Phys. Commun.* **91**, 43–56 (1995).
30. Daura, X. *et al.* Parametrization of aliphatic CH_n united atoms of GROMOS96 force field. *J. Comput. Chem.* **19**, 535–547 (1998).